Acta Geodyn. Geomater., Vol. 23, No. 1 (221), 111–128, 2026
DOI: 10.13168/AGG.2026.0007
journal homepage: https://www.irsm.cas.cz/acta

ORIGINAL PAPER

PRESSURE RELIEF, SHOCK ABSORPTION, AND ENERGY ABSORPTION EFFECTS OF PROTECTIVE LAYER MINING

Jinzheng BAI [1,2,3,4,5] *, Linming DOU [2, 3], Siyuan GONG [2, 3], Anye CAO [2, 3], Xiufeng ZHANG [4, 5], Leigang MIAO [1] and Hongjun GUO [1]

1) Jiangsu Vocational Institute of Architectural Technology, Xuzhou, PR China
[2] School of Mines, China University of Mining and Technology, Xuzhou, PR China
[3] State Key Laboratory for Fine Exploration and intelligent Development of Coal Resources, China University of Mining and Technology, Xuzhou, PR China
[4] Research Center for Rock Burst Control, Shandong Energy Group Co., Ltd., Jinan, PR China
[5] Key Laboratory of Coal Mine Rock Burst Prevention & Control Technology and Equipment, National Mine Safety Administration, Jinan, PR China

**Corresponding author's e-mail:* baijinzheng@cumt.edu.cn

ARTICLE INFO

Article history:
Received 11 December 2025
Accepted 24 January 2026
Available online 5 February 2026

Keywords:
Rock burst
Protective seam mining
Pressure relief
Energy absorption
Prevention effectiveness

ABSTRACT

Protective layer mining represents one of the most effective and economical regional strategies for rock burst prevention. Studying its anti-impact mechanisms carries significant scientific implications and provides substantial guidance for engineering applications. This study systematically investigates the pressure relief, vibration damping, and energy absorption effects of protective layer mining by integrating theoretical analysis, numerical simulation, and engineering practice. The results demonstrate that, within a certain temporal and spatial range after protective layer extraction, both the stress and abutment pressure in the protected layer are markedly reduced, with a stress reduction rate reaching up to 25 %. Additionally, the frequency and intensity of dynamic loads induced by the fracture and slip of overlying strata are substantially attenuated. The loose and fragmented structures formed by protective layer mining effectively dampen far-field mining seismicity. Furthermore, following the prior extraction of the protective layer, the incremental strain energy near the working face during the mining of the protected layer is significantly decreased. The effectiveness of protective layer mining in mitigating rock burst hazards is closely related to factors such as interburden spacing, lithology of intervening strata, and coal seam thickness. Building upon these findings and contextualized within a developing mine, a design scheme for protective layer mining is proposed, laying a solid stress foundation for reducing the rock burst risk in the protected layer.

1. INTRODUCTION

In recent years, with the increasing mining depth and intensity, both the frequency and severity of rock burst accidents have risen sharply. Rock burst has become one of the most critical dynamic hazards in deep coal mining, posing serious threats to the exploitation of deep energy, mineral resources, and underground space in China (Dou et al., 2022; Cook, 1965). According to the "Detailed Rules for Preventing and Controlling Rock burst in Coal Mines" issued by China's National Coal Mine Safety Administration in 2019, "the feasibility of protective layer mining shall be comprehensively evaluated based on factors such as interlayer spacing, coal seam thickness, and the burst tendency of coal seams and their surrounding rock. Where conditions permit, protective layer mining must be implemented." Given the complex geological conditions of China's coal resources, extensive engineering practice has demonstrated that protective layer mining stands as one of the most effective and economical regional strategic measures for rock burst prevention (Xie et al., 2011; Liu et al., 2010; Ellsworth, 2013). Therefore, investigating the pressure-relief, shock-absorption, and energy-absorption effects of protective layer mining holds significant scientific importance and provides valuable guidance for engineering practice.

From the perspective of rock burst prevention, a protective layer is defined as a coal seam that is mined in advance to eliminate or mitigate the rock burst risk in adjacent seams (Sun et al., 2016). The historical progression of this technology is notable: initially applied in France in the 1930s for gas outburst control, protective layer mining was subsequently adopted in major coal-mining countries prone to rock burst, including Czechoslovakia, the former Soviet Union, South Africa, Germany, and Poland (Noack et al., 1998). In China, practical research on protective layer mining commenced in 1958, achieving significant outcomes in mines such as Beipiao, Tianfu, Nantong, Zhongliangshan, Songzao, Xishan, Huajin, Tiefa, and Huaibei (Wang et al., 2017). Notably, field trials at the Mentougou Mine demonstrated its effectiveness in suppressing rock burst, accumulating valuable empirical data. The traditional mechanism primarily relied on the natural emission of pressure-relieved gas through mining-induced fractures to eliminate outburst risks (Yuan et al., 2014). With

Cite this article as: Bai J, Dou L, Gong S, Cao A, Zhang X, Miao L, Guo H: Pressure relief, shock absorption, and energy absorption effects of protective layer mining. Acta Geodyn. Geomater., 23, No. 1 (221), 111–128, 2026. DOI: 10.13168/AGG.2026.0007

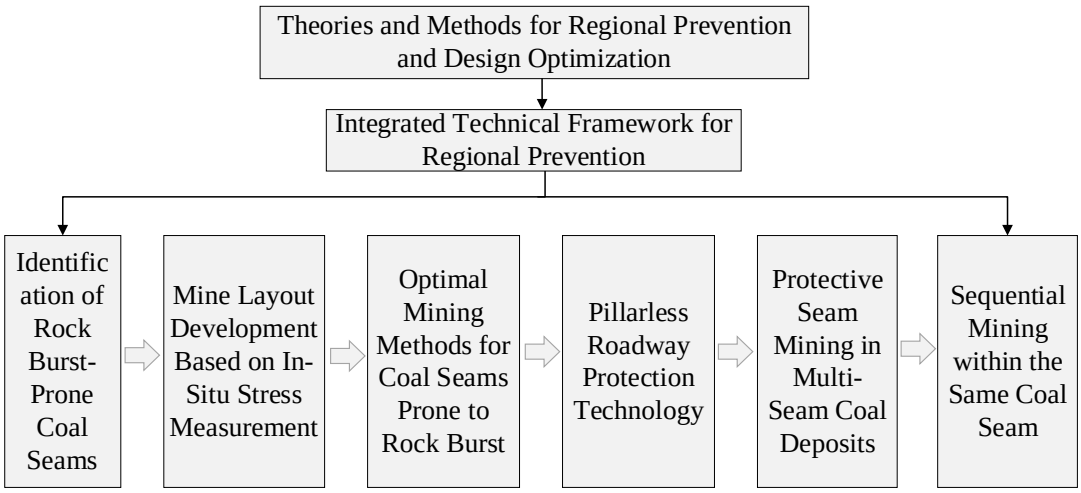

Fig. 1 Technical framework for regional rock burst prevention and control.

further development, the technical scope has broadened, now encompassing dual-core objectives: pressure relief for rock burst prevention in the protected layer and enhanced gas extraction for outburst prevention.

Regarding the rock burst prevention effect of protective layer mining, scholars domestically and internationally have primarily converged on two key scientific issues: the "extent of the pressure-relief zone created by protective layer mining" and the "pressure-relief and movement patterns of the protected coal-rock mass." Research approaches encompassing field observation (Yang et al., 2011; Liu et al., 2013), theoretical analysis (Wang et al., 2011; Yin et al., 2017), physical similarity simulation (Zhao et al., 2023; Jiao et al., 2017), numerical simulation (Tu et al., 2017; Jiang et a., 2019), and experimental studies (Fang et al., 2021) have yielded substantial findings. For instance, based on the relationship between normal stress and permeability, the coal-rock mass beneath the protective layer has been categorized into a model of "three horizontal zones and three vertical bands" (Yardimci et al., 2020). Tracer gas has been employed to measure the development timing, location, and extent of inter-layer through-going fractures, validating quantitative calculations of floor failure depth and qualitatively analyzing their impact on gas migration and extraction in closely spaced coal seams (Qi et al., 2014). Other studies have investigated the meso-damage and permeability evolution of the unloaded coal mass in the protected layer (Yuan et al., 2008), proposed new methodologies for determining the protective scope via flow observation and numerical simulation (Tian et al., 2013), and revealed the rock burst prevention mechanism of underlying protective layers (Dai et al., 2025). In summary, existing research has focused on the influence of static mining-induced stress, largely overlooking the dynamic disturbance effects from mining-induced seismicity during actual extraction processes. Given that rock burst is widely recognized as a result of the combined action of static and dynamic loads, it remains imperative to further investigate the anti-impact efficacy of protective layer mining under the coupled stress paths of real static mining-induced stress and dynamic disturbance. Such research is crucial for advancing the application of protective layer mining technology in China and achieving proactive regional rock burst prevention.

In this context, this study systematically proposes a pressure-relief, shock-absorption, and energy-absorption rock burst prevention mechanism for protective layer mining. The scientific implementation of this technique can substantially reduce the regional risk of rock burst during mining operations. Subsequently, the key spatio-temporal factors influencing the effectiveness of protective layer mining in preventing rock burst were investigated through numerical simulation. Finally, the proposed mechanism was validated via field application of the research findings, confirming its rationality.

2. THEORETICAL BASIS OF ROCK BURST PREVENTION IN PROTECTIVE SEAM MINING

2.1. PREVENTION AND CONTROL STRATEGIES FOR ROCK BURST IN PRONE AREAS

The prevention and control of rock burst should adhere to the principle of "regional measures first, local measures follow-up, zoned management, and categorized prevention" (Regulations on the Prevention and Control of Rock Burst in Coal Mines, 2019). A significant cause of rock burst incidents is the insufficient systematic approach to burst prevention during the initial design phase of mine field planning, which limits the effectiveness of subsequent local control and individual protective measures. As illustrated in Figure 1, the regional prevention strategy aims to fundamentally mitigate rock burst risks by optimizing mine design philosophy and implementing comprehensive regional control measures.

The occurrence of rock burst is closely associated with the regional stress field and localized

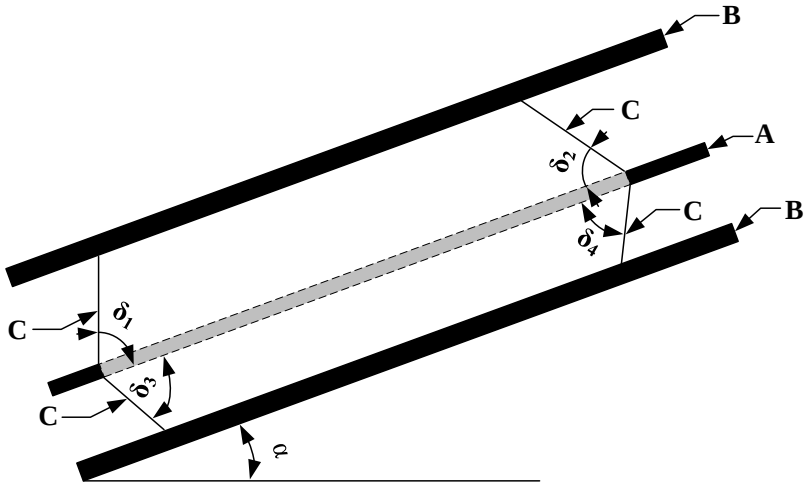

A—Protective seam; B—Protected seam; C—Boundary of the protected area;
δ_1、δ_2、δ_3、δ_4—The relief angles along various orientations

Fig. 2 The protective range of the protective seam working face along the inclined direction.

stress concentrations induced by mining activities. Regional rock burst prevention measures are instrumental in mitigating stress levels at the source, thereby reducing the overall risk of rock burst. These measures primarily encompass two aspects. First, measures aimed at preventing regional rock burst hazards through optimized mining design, including but not limited to: development layout, mining and excavation deployment, extraction sequences in multi-seam mining, selection of protective seams, sequential extraction of working faces, design of coal pillar dimensions, positioning and horizon selection of main roadways, as well as choices of mining methods and techniques. Second, preventive measures implemented on a regional scale to weaken coal-rock masses and alleviate stress levels, such as coal seam water infusion, comprehensive pre-decompression of coal bodies across the region, and pre-splitting of roof strata.

For regional rock burst prevention measures aimed at optimizing mining design, primary consideration should be given during the mine design and panel layout planning stages. In contrast, preventive measures designed to weaken coal-rock mass and reduce stress levels on a regional scale are primarily implemented before roadway development or prior to longwall face extraction. Consequently, the key advantage of regional prevention strategies lies in their proactive implementation before mining activities commence in burst-prone coal seams. This approach ensures that rock burst prevention efforts do not interfere with extraction operations in high-risk zones, while generally delivering more effective outcomes compared to localized control measures.

As the most effective strategic measure for regional rock burst prevention, protective layer mining should first be assessed for feasibility based on factors such as interlayer spacing, coal seam thickness, and the burst tendency of the coal seam and its roof and floor when extracting coal seam groups in burst-prone mines. If feasible, priority should be given to selecting coal seams with no burst tendency or low burst risk as the protective layer.

2.2. PROTECTION ZONE OF PROTECTIVE SEAM MINING

The protective range of protective seam mining refers to the area within which the rock burst risk in the protected coal seam is eliminated or significantly reduced due to the spatial effects induced by the extraction of the protective seam (Wu et al., 2012). When mining a protective seam for the first time in a mine, reasonably determining its protective range is of significant guiding importance for scientifically and rationally arranging working faces to achieve an optimal protective effect.

The protective range of the protective seam should be determined based on the pressure relief angle δ, as illustrated in Figure 2. The pressure relief angle δ is related to the coal seam inclination angle α, with the corresponding relationship detailed in Table 1.

The maximum vertical protective spacing between the protective layer and the protected layer can be determined with reference to Equation (1), Equation (2), or Table 2.

Maximum effective distance of the underlying protective layer:

$$S_{Underlying} = S'_{Underlying}\beta_1\beta_2 \quad (1)$$

Maximum effective range of the upper protective layer:

$$S_{Upper} = S'_{Upper}\beta_1\beta_2 \quad (2)$$

Table 1 Pressure relief angle of the protective layer along the dip direction.

Coal 0seam dip α/°	Pressure relief angle δ/°			
	δ_1	δ_2	δ_3	δ_4
0	80	80	75	75
10	77	83	75	75
20	73	87	75	75
30	69	90	77	70
40	65	90	80	70
50	70	90	80	70
60	72	90	80	70
70	72	90	80	72
80	73	90	78	75
90	75	80	75	80

Table 2 The effective vertical distance between the protective layer and the protected layer.

Coal seam type	Maximum effective vertical distance /m	
	Upper protective layer	Underlying protective layer
Steeply inclined coal seam	＜60	＜80
gently inclined and inclined coal seams	＜50	＜100

Table 3 The geological occurrence and mechanical parameters of coal and rock strata.

Lithology	Layer thickness/ m	Poisson's ratio/u	Unit weigh /kN·m^{-3}	Elastic modulus/GPa	Bulk modulus/GPa	Shear modulus/GPa	Cohesion /MPa	Internal friction angle /°
Sandy mudstone	22	0.26	26.50	7.37	5.12	2.92	1.90	35.73
Siltstone	12	0.24	25.90	7.02	4.50	2.83	2.08	39.40
Sandy mudstone	21	0.26	26.50	7.37	5.12	2.92	1.90	35.73
Fine-grained sandstone	21	0.22	25.90	13.08	7.79	5.36	2.59	39.74
Sandy mudstone	11	0.26	26.50	7.37	5.12	2.92	1.90	35.73
No. 2-2 seam	3	0.26	13.30	6.84	4.75	2.71	1.98	35.84
Sandy mudstone	11	0.26	26.50	7.37	5.12	2.92	1.90	35.73
Fine-grained sandstone	11	0.22	25.90	13.08	7.79	5.36	2.59	39.74
Sandy mudstone	19	0.26	26.50	7.37	5.12	2.92	1.90	35.73
No. 3-1 seam	6	0.26	13.30	6.84	4.75	2.71	1.98	35.84
Sandy mudstone	14	0.26	26.50	7.37	5.12	2.92	1.90	35.73
Fine-grained sandstone	19	0.22	25.90	13.08	7.79	5.36	2.59	39.74

In the equation, $S'_{Underlying}$ and S'_{Upper} denote the theoretical effective vertical distances to the lower and upper protective layers, respectively. These distances are related to the working face length L and mining depth H, and their values can be determined with reference to Table 3. When L>0.3 H, L shall be taken as 0.3 H, however, the value of L must not exceed 250 m.

In the equation: β_1 is the influence coefficient of protective seam mining.

When $M \leq M_0$, $\beta_1 = M/M_0$; when $M > M_0$, $\beta_1 = 1$. Here, M denotes the mining thickness of the protective seam (in meters), and M_0 represents the minimum effective thickness of the protective seam (in meters). β_2 is the coefficient of hard interlayer rock (e.g., sandstone, limestone) content, expressed as η, which indicates the percentage of hard rock within the interlayer strata. When η > 50 %, $\beta_2 = 1–0.4\eta/100$; when $\eta \leq 50$ %, $\beta_2 = 1$.

2.3. PRESSURE RELIEF, VIBRATION DAMPING, AND ENERGY ABSORPTION EFFECTS FOR ROCK BURST PREVENTION

Research indicates (Wu et al., 2012) that the occurrence of rock burst must satisfy the following three conditions: the strength condition (i.e., the stress exerted on the coal-rock mass must exceed its strength

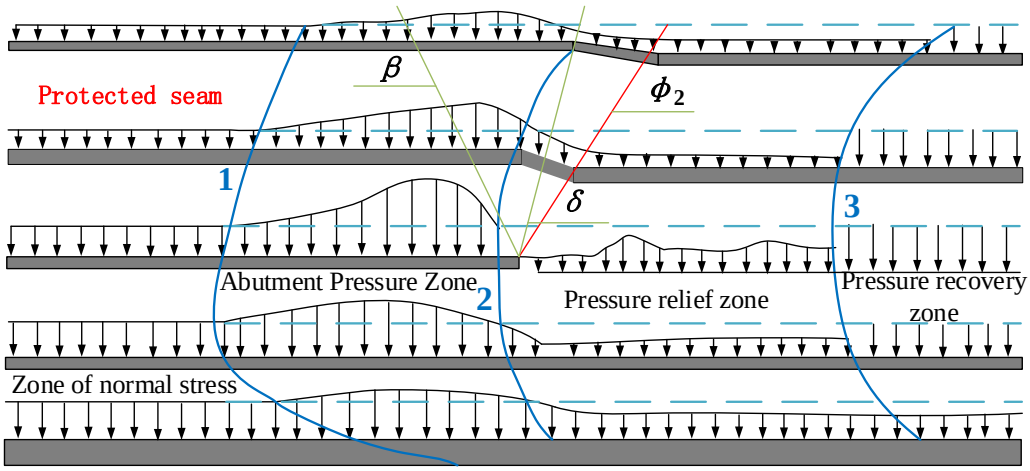

Fig. 3 Pressure-relief effect of protective seam mining.

to initiate failure), the energy condition (i.e., energy must continuously accumulate within the coal-rock mass and be capable of sudden release), and the burst tendency of the coal-rock mass (i.e., its capacity to undergo brittle failure). Among these, burst tendency is an inherent property of the coal-rock mass and cannot be altered artificially. However, mining protective coal seams reduces the stress on the coal-rock mass, releases the elastic energy stored in the roof and floor strata, and minimizes vibrations induced by roof fracturing. Meanwhile, the loose, weak structures formed after protective seam mining effectively absorb dynamic load disturbances generated by far-field seismic events. As a result, the simultaneous satisfaction of the three aforementioned conditions is prevented, thereby averting dynamic rock burst disasters and providing protective and liberating effects for the mining of underlying protected seams. This mechanism constitutes the pressure-relief, vibration-damping, and energy-absorbing rock burst prevention effect of protective seam mining.

Pressure relief is the primary objective of implementing protective seam mining. As shown in Figure 3, the extraction of the protective seam induces deformation, fracturing, separation, and displacement of the surrounding rock toward the mined-out area. Based on the degree and characteristics of disturbance caused by protective seam mining on the coal-rock mass, the stress distribution along the strike or dip direction can be categorized into four zones: the normal stress zone, the abutment pressure zone, the pressure relief zone, and the stress recovery zone. These four stress distribution patterns advance in the same direction as the working face of the protective seam, progressively exerting varying degrees of influence on the protected seam. The normal stress zone remains unaffected by mining activities. The extent of the abutment pressure zone depends on factors such as mining depth, working face length, coal seam thickness, and inclination. In the pressure relief zone, stress is transferred to the coal and rock layers beyond this zone, resulting in a continuous reduction of pressure on the coal mass. This pressure reduction effect causes the coal mass to undergo expansive deformation, releasing elastic energy. As a result, the protected seam is liberated and loses its potential for rock burst. In the stress recovery zone, the stress level remains lower than the original in-situ stress, and the coal seam retains some degree of expansive deformation, maintaining a state of pressure relief and protection.

As illustrated in Figure 4, the protective layer mining achieves its vibration reduction effect primarily through two mechanisms: First, the extraction of the protective layer reduces the likelihood of large-energy seismic events induced by overburden rock failure, with the predominant seismic activity shifting towards small- to medium-energy mine tremors that pose a lesser threat to roadway stability. Second, the loose and fractured structure generated by the mining process effectively attenuates far-field mine tremors. This mechanism fundamentally minimizes the risk of rock burst that could be triggered by the superposition of roof-type mine tremor stress waves with the in-situ stress field exceeding the ultimate strength of the coal and rock mass surrounding the roadway. Consequently, this dual mechanism provides robust protection for the safe extraction of the protected working face.

As shown in Figure 5, when seismic waves propagate through different media, the vibration energy attenuates in a power-law relationship with increasing propagation distance. The attenuation is relatively minor in media with good integrity and continuity, such as cement ground and compacted gravel ground. In contrast, greater attenuation occurs in loose and highly porous media, such as sandy soil or fields of small stones. This indicates that fractures, joints, and pores within the propagation medium significantly absorb and dampen seismic wave energy. Furthermore, this effect varies with the integrity, hardness, porosity, and other properties of the medium: the more favorable these properties are, the smaller the attenuation exponent becomes, and vice versa.

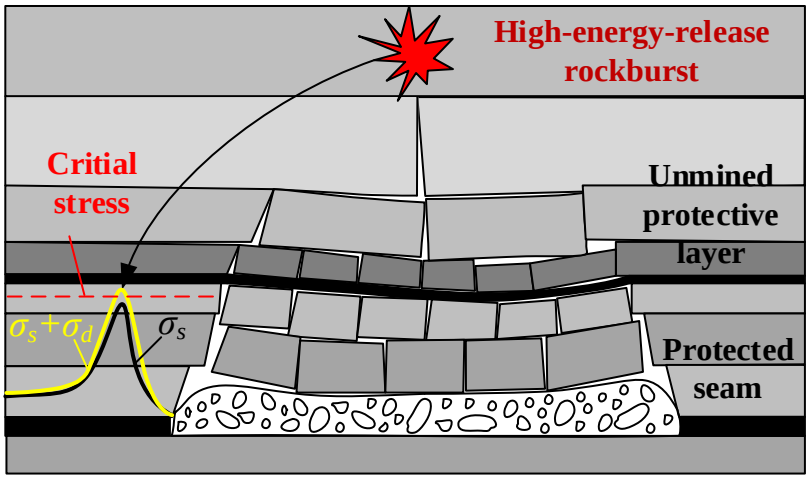

(a) Unmined protective layer

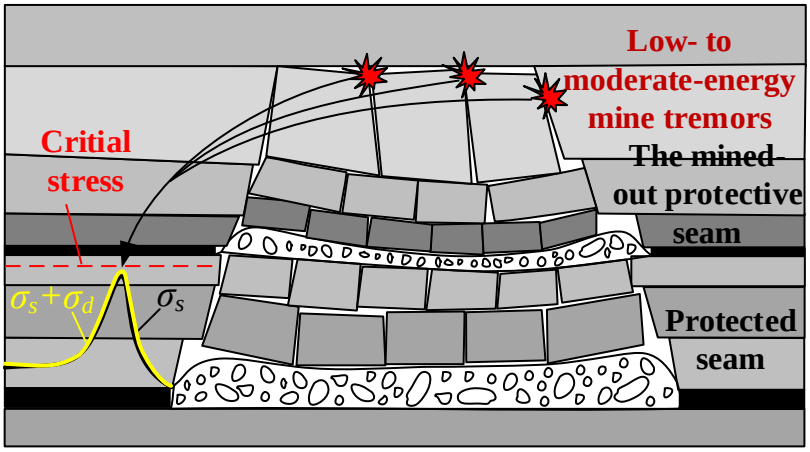

(a) The mined-out protective seam

Fig. 4 Seismic attenuation effects induced by protective layer mining.

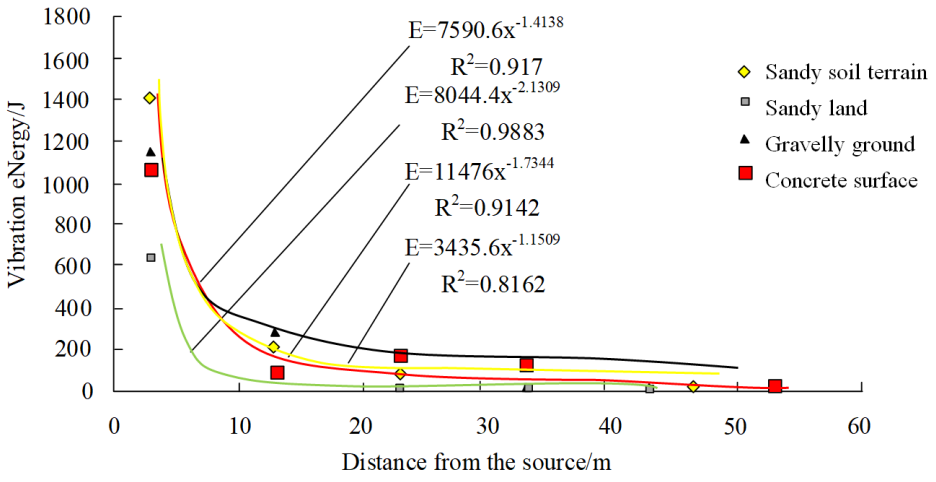

Fig. 5 The energy-absorbing effect of protective layer mining.

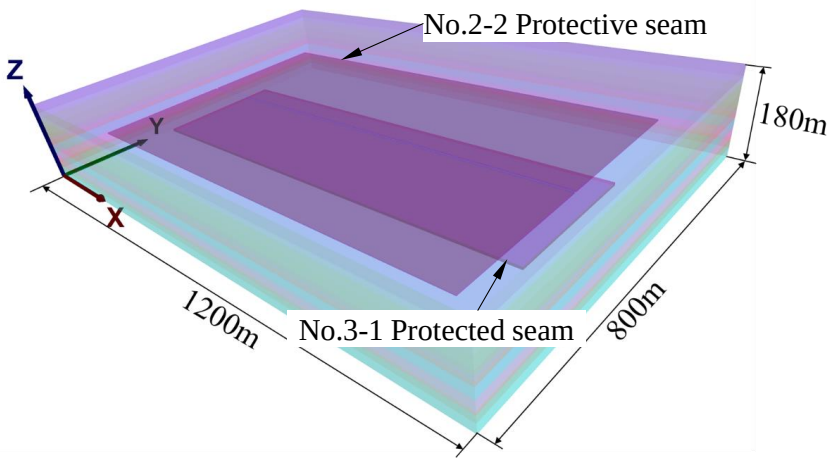

Fig. 6 he protective seam mining-induced liberation system model.

3. NUMERICAL SIMULATION VERIFICATION OF THE ROCK BURST PREVENTION EFFECT IN PROTECTIVE SEAM MINING

3.1. NUMERICAL MODEL

Based on the geological conditions of a newly constructed deep rock burst-prone mine in Western China, by establishing a protective layer mining-induced stress relief system model, as illustrated in Figure 6, which comprises overlying strata, protective layer, intermediate strata, protected layer, and floor strata, the pressure reduction, vibration attenuation, and energy absorption effects associated with protective layer mining were validated through simulations conducted with FLAC^{3D} software.

The model simulated Protective Seam 2-2 with a burial depth of 680 m and a coal thickness of 3 m. The protected seam (Seam 3-1) has a thickness of 6 m, and the interburden spacing between the two seams is 41 m. The model dimensions are 1200 m (strike) × 800 m (dip) × 180 m (vertical). The overlying rock stratum above the protective seam is 87 m thick, while the floor stratum is 33 m thick. The boundary conditions for the model are defined as follows: the bottom boundary is fixed, the lateral boundaries are simply supported, and the lateral pressure coefficient is set to 1.0. A uniformly distributed equivalent load of 15 MPa is applied to the top of the model. The physical and mechanical parameters of the coal and rock selected for the numerical calculation model are listed in Table 3. The strike length of the protective seam working face is 400 m with a dip width of 200 m. Each excavation step advances 4 m, and the simulation was run for 3000 calculation steps.

3.2. THE PRESSURE-RELIEF EFFECT OF PROTECTIVE SEAM MINING

Figure 7 illustrates the distribution patterns of three-dimensional stresses along the vertical direction following the extraction of the protective coal seam. It can be observed that the variations in triaxial stresses do not exhibit a linear relationship with increasing distance from the protective seam.

After the extraction of the protective seam, the triaxial stresses in its vicinity are reduced to nearly zero. The general pattern observed is as follows: 1) The closer to the 2–2# coal protective seam, the lower the triaxial stresses; conversely, stresses increase with distance, indicating a diminishing protective effect. The recovery rate of horizontal stress differs significantly from that of vertical stress. 2) Within 16 m above the protective seam roof, the region lies in the caved zone where vertical stress is essentially zero. Within 70 m above the roof and 72 m below the floor of the protective seam, the area falls within the effective pressure-relief range, where triaxial stresses are all lower than the original rock stress. This provides favorable mechanical conditions for mining the protected seam. 3) At the location of the 3–1# protected seam, the triaxial stresses are approximately equal, about 13.5 MPa, whereas the original rock stress at this location is about 18 MPa. Thus, the stress release rate induced by protective seam mining is approximately 25 %, demonstrating the pressure-reduction effect of protective seam extraction on the protected seam.

Figure 8 presents the vertical stress increment nephograms at different strata after the extraction of the protected coal seam. The general patterns are as follows: 1) As shown in Figure 8(a), the stress surrounding the gateways adjacent to the working face in the protective seam is relatively low, forming an “O”-shaped pressure-relief zone around the goaf. 2) As illustrated in Figure 8(b), within the pressure-relief zone near the protective seam, the vertical stress measures approximately 9 MPa, which is lower than the in-situ stress at this stratum. 3) With increasing vertical distance, as depicted in Figures 8(c) to (d), the “O”-shaped pressure-relief zone gradually contracts away from the coal seam, leading to a progressive weakening of the pressure-relief effect.

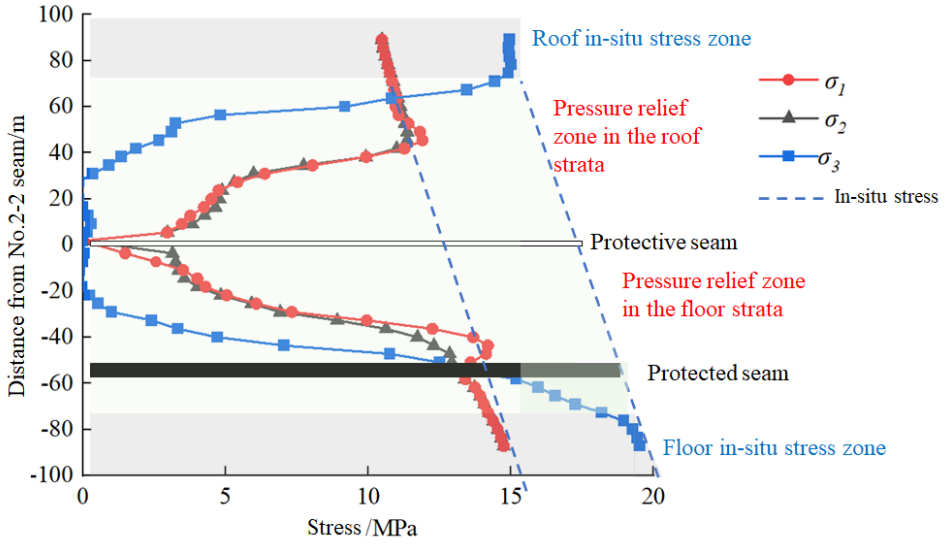

Fig. 7 Three-dimensional vertical stress distribution diagram following protective seam mining.

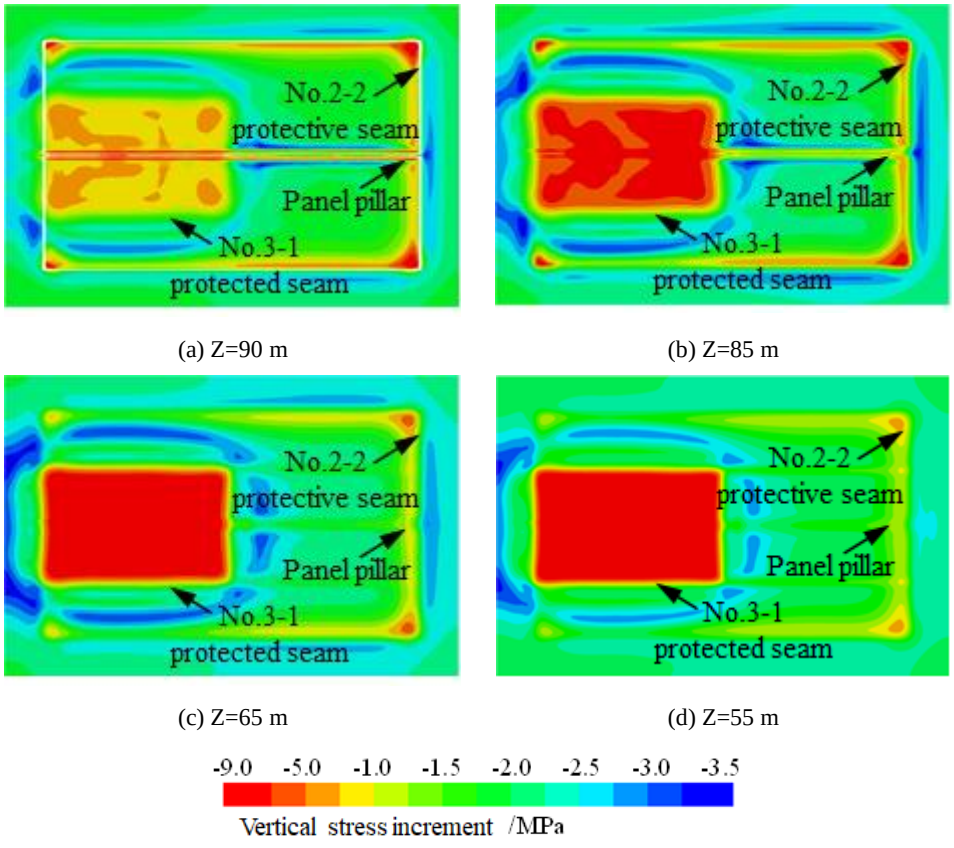

Fig. 8 Vertical stress increment contour maps at various stratigraphic levels following the extraction of the protected coal seam.

3.3. THE WAVE-DAMPING EFFECT OF PROTECTIVE SEAM MINING

Based on actual mine seismic signals obtained from the in-situ SOS microseismic monitoring system, a dynamic load was applied to fine-grained sandstone 20 meters above the 2-2 coal seam to simulate roof fracturing. The load time-history of the corresponding stress wave is shown in Figure 9. The peak amplitude of the dynamic load signal is approximately 0.6 mm/s, with a peak stress of about 60 MPa and a signal

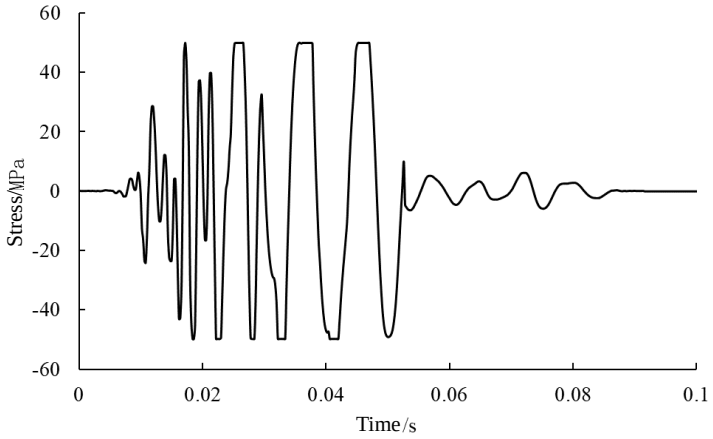

Fig. 9 Dynamic stress wave loading time history.

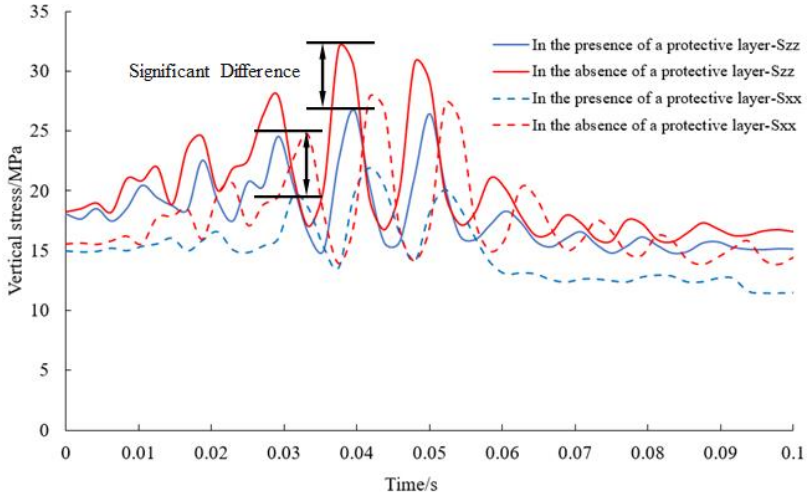

(a) Stress response characteristics

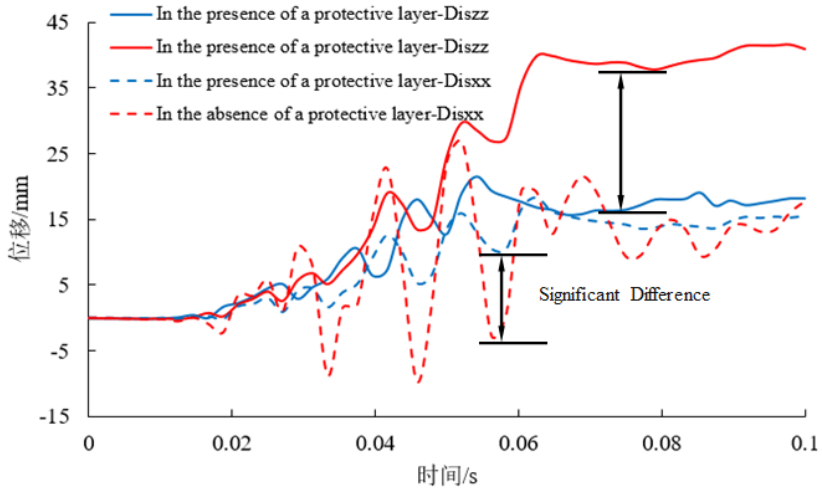

(b) Displacement response characteristics

Fig. 10 Response characteristics of stress and displacement.

duration of approximately 0.3 seconds. Monitoring points were arranged in the protected coal seam roadway directly beneath the seismic source. A comparative analysis was conducted on the stress and displacement response characteristics of the surrounding rock in the protected seam roadway undermine seismic disturbances, with and without protective layer mining, as illustrated in Figure 10.

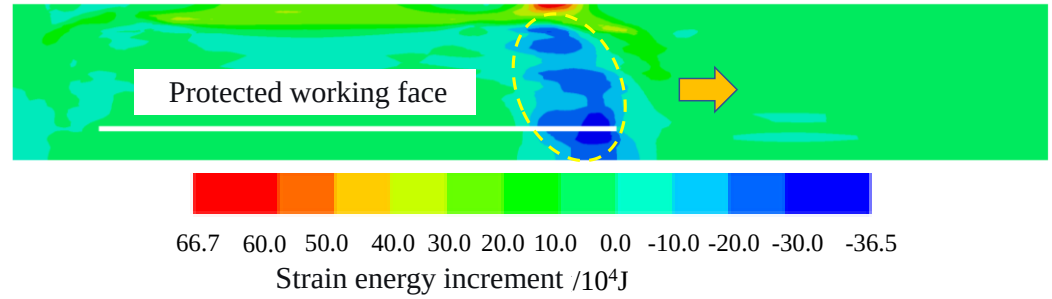

(a) In the presence of a protective layer

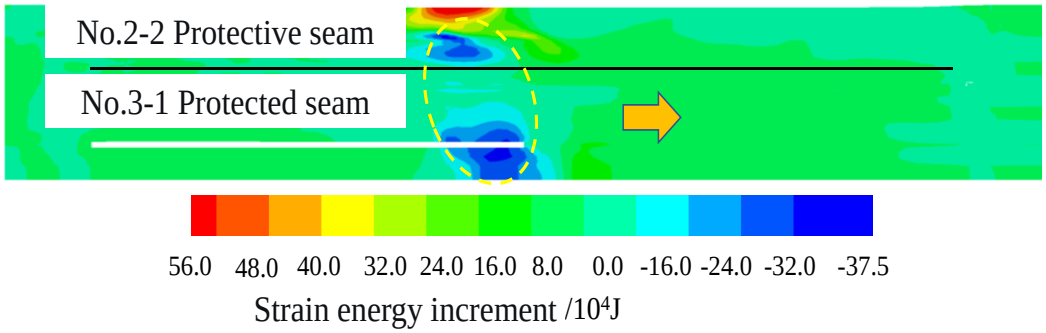

(b) In the absence of a protective layer

Fig. 11 Cloud map of strain energy increment along the dip direction.

In general, when dynamic loads propagate to the vicinity of the protected layer, both vertical and horizontal stresses exhibit oscillatory increases until reaching peak values. Subsequently, the stresses gradually attenuate within the time interval of 0.06–0.08 s, leading to the stabilization of the coal-rock mass.

As illustrated in Figure 10(a), prior to the extraction of the protective layer, the peak vertical stress in the roof of the protected coal seam induced by dynamic loading reached 32.6 MPa. Following the extraction of the protective layer, the peak vertical stress resulting from the same dynamic loading decreased to 27.5 MPa, representing a reduction of approximately 15.6 %. Correspondingly, prior to protective layer extraction, the peak horizontal stress induced by dynamic loading was 28.6 MPa. After extraction, this value declined to 22.8 MPa, corresponding to a reduction of approximately 20.3 %.

As shown in Figure 10(b), prior to protective layer extraction, the peak vertical displacement in the roof of the protected layer induced by dynamic loading reached 42.5 mm. After extraction, the peak vertical displacement due to the same loading decreased to 23.8 mm, representing a reduction of approximately 36.9 %. Similarly, prior to extraction, the peak horizontal displacement induced by dynamic loading was 26.2 mm, which declined to 17.8 mm after extraction, corresponding to a reduction of approximately 34.4 %.

The above findings demonstrate that the plastic failure zone generated after protective layer extraction exhibits a significant damping effect on both stress and displacement in the protected layer induced by dynamic disturbances. Moreover, the extraction of the protective layer provides a more pronounced damping effect on the peak horizontal stress and displacement of the surrounding rock under dynamic loading compared to the corresponding vertical stress and displacement peaks.

3.4. THE ENERGY-ABSORBING EFFECT OF PROTECTIVE SEAM MINING

In this paper, the energy-absorbing effect of protective seam mining refers to the process in which the caved and fractured zones formed after protective seam excavation disrupt the intact structure of surrounding coal-rock masses, thereby increasing the attenuation coefficient of seismic wave propagation and consequently absorbing vibrational energy. Figure 11 presents a comparison of the incremental strain energy along the strike direction of the model with and without protective seam mining. The calculation method involves subtracting the overall strain energy of the surrounding rock in its initial state from that after the mining of the protected seam. Thus, a positive value indicates the accumulation of elastic strain energy during the mining process, while a negative value signifies the release of elastic strain energy, which corresponds to a higher risk of rock burst.

As illustrated in Figure 11, prior to the extraction of the protective layer, a notable strain energy release zone is observed ahead of the working face in the protected layer, extending from the roof of the protective layer to the floor region of the protected layer, with a peak strain energy release of approximately 3.65E+05 J. Following the extraction

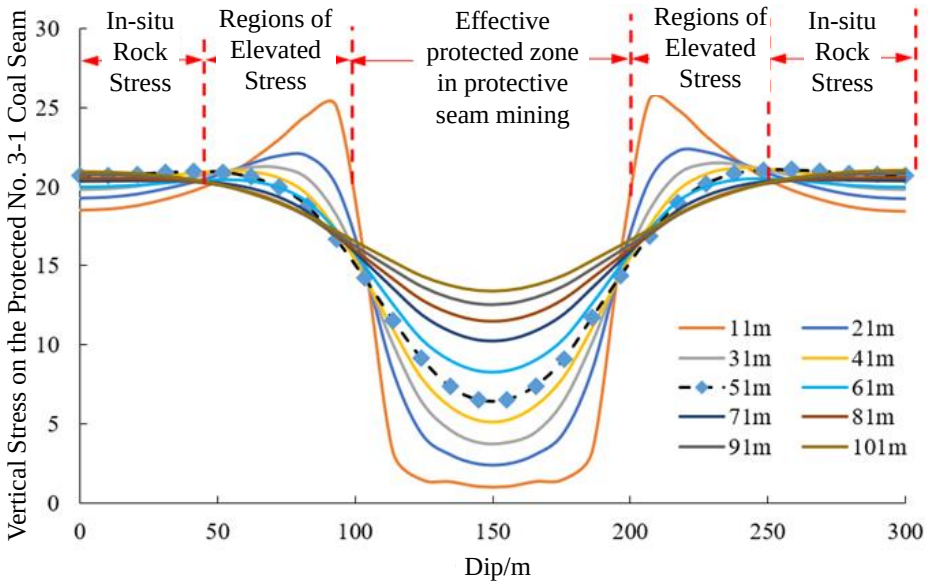

Fig. 12 Vertical stress of roof with different seam spacing.

of the protective layer, the strain energy release zones are predominantly distributed in two distinct areas: one above the protective layer and another in proximity to the protected layer. Although the peak strain energy release measures approximately 3.75E+05 J, slightly higher than that in the absence of the protective layer, the spatial extent of these zones is significantly reduced, particularly within the interlayer rock strata, where elastic strain energy variations stabilize. This indicates that subsequent extraction of the protected layer, after prior extraction of the protective layer, results in a marked reduction in both the spatial scope and magnitude of strain energy increments in the area ahead of the working face. The integrity of the coal-rock mass is effectively compromised, thereby weakening the geological conditions conducive to rock burst initiation. Consequently, the potential and associated risks of dynamic hazards such as rock burst are eliminated. These findings demonstrate that the extraction of the protective layer effectively dissipates energy and mitigates stress disturbances induced by mining activities.

4. ANALYSIS OF INFLUENCING FACTORS ON THE EFFECTIVENESS OF PROTECTIVE SEAMS IN ROCK BURST PREVENTION

The results indicate that the scope and intensity of the depressurization-damping-energy absorption effects provided by protective seam mining on the protected seam are closely correlated with the interburden spacing, lithological characteristics, and seam thickness. Qualitatively, the rock burst prevention efficacy of protective seam mining is characterized by stress reduction and displacement increase. Quantitatively, however, the extent of such stress and displacement variations remains to be precisely determined. Therefore, the focus of protective seam mining lies in evaluating the depressurization-damping-energy absorption effects on the protected seam after the extraction of the protective seam, as well as assessing the effectiveness of these effects.

4.1. INTER-SEAM SPACING

The initial interlayer distance in the protective seam mining pressure relief system model is set at 31 m. A comparative analysis was conducted to examine the vertical stress distribution in the roof of the protected seam along the inclined cross-section of the model after mining the protective seam face, with interlayer distances of 11 m, 21 m, 31 m, 41 m, 51 m, 61 m, 71 m, 81 m, 91 m, and 101 m. The results are illustrated in Figure 12.

As can be seen from Figure 12, the area directly beneath the goaf of the protective layer constitutes the most effective protection zone with the most pronounced pressure relief effect. Extending outward on both sides of the working face are the stress elevation zone and the original rock stress zone, respectively. Within the effective protection zone, a smaller interlayer distance between coal seams corresponds to a more significant reduction in vertical stress. When the interlayer distance is 11 m, the vertical stress at the roof of the protected layer is approximately 3.5 MPa. In contrast, when the interlayer distance increases to 101 m, the vertical stress rises to about 15 MPa. However, an excessively close interlayer distance can also exacerbate the vertical stress concentration on both sides of the working face goaf. This indicates that when the interlayer distance is too small, the dynamic disturbance induced by protective layer mining will severely compromise the stability of the surrounding rock in the protected layer working face.

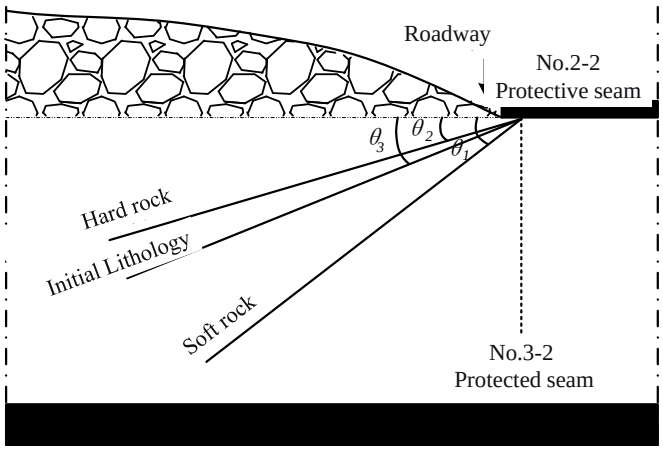

Fig. 13 The influence of different inter-lithology on critical relief angle.

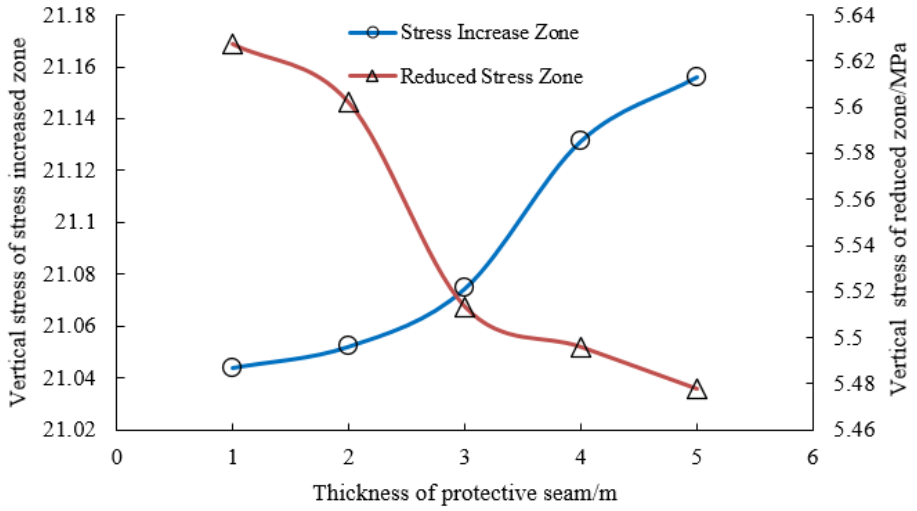

Fig. 14 Peak stress for different protective seam thicknesses.

4.2. INTERLAYER LITHOLOGY

According to relevant research, the lithology of the intervening strata has a significant influence on the extraction of the protective layer, primarily through rock mechanics parameters such as the elastic modulus, bending and shear strength, Poisson's ratio, cohesion, and unit weight of the rock mass. In the model of the protective layer mining-induced pressure relief system, the initial interlayer lithology is dominated by sandy mudstone. A comparative analysis is conducted to examine the impact on the critical pressure relief angle for the underlying protected layer when the interlayer lithology is changed to mudstone, fine sandstone, and siltstone, respectively.

Due to the weak mechanical properties of soft rock, the depth at which plastic deformation and failure occur in the interlayer rock mass beneath the goaf is relatively large. After plastic failure, the maximum depth of soft rock extends all the way to the coal seam of the protected layer. In contrast, hard rock exhibits higher strength, and the depth of plastic failure in the interlayer rock mass generally develops and remains confined within a specific lithological stratum.

As shown in Figure 13, the maximum critical pressure relief angle θ_1 for soft rock, represented by mudstone and sandy mudstone, is 37°. The maximum critical pressure relief angle θ_2 for hard rock, represented by fine sandstone, coarse sandstone, and siltstone, is 16°. The maximum critical pressure relief angle θ_3 for the original interlayer lithology, dominated by sandy mudstone and fine-grained sandstone, is 22°. Consequently, under mining-induced disturbance, the critical pressure relief angle for plastic deformation and failure in soft rock is greater than that for hard rock under the same conditions.

4.3. COAL SEAM THICKNESS

4.3.1. DIFFERENT PROTECTIVE SEAM THICKNESS

In the pressure relief system model for protective layer mining, the initial protective seam thickness is set at 3 m. A comparative analysis was conducted to examine the influence of protective seam thicknesses of 1 m, 2 m, 3 m, 4 m, and 5 m on the vertical stress at the roof of the protected layer after mining the protective layer. The results are shown in Figure 14.

As shown in Figure 14, the peak vertical stress in both the stress concentration zone and the pressure

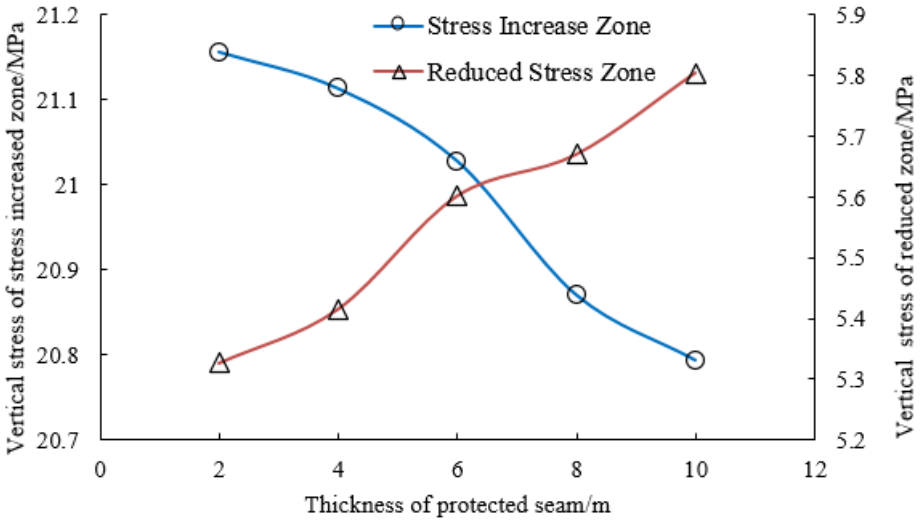

Fig. 15 Peak stress for different protected seam thicknesses.

relief zone at the roof of the protected layer does not vary significantly with different protective seam thicknesses. When the protected seam thickness is 6 m and the protective seam thickness is 1 m, the peak stress in the pressure relief zone is approximately 5.6 MPa, while that in the stress concentration zone is about 21 MPa. When the protected seam thickness remains unchanged and the protective seam thickness increases to 5 m, the peak stress in the pressure relief zone is approximately 5.4 MPa, and that in the stress concentration zone is about 21.2 MPa. Therefore, as the protective seam thickness increases, the peak stress in the pressure relief zone gradually decreases, whereas the peak stress in the stress concentration zone gradually increases.

4.3.2. DIFFERENT PROTECTED SEAM THICKNESS

In the model of protective layer mining for pressure relief, the initial thickness of the protected stratum is set as 6 m. A comparative analysis is conducted to examine the influence of protective layer mining operations on the vertical stress at the roof of the protected stratum when its thickness varies as 2 m, 4 m, 6 m, 8 m, and 10 m. The results are presented in Figure 15.

As illustrated in Figure 15, the peak vertical stresses in both the stress-relieved zone and the stress-concentrated zone at the roof of the protected layer show little variation with changes in the thickness of the protected layer. When the protective layer is 3 m thick and the protected layer is 2 m thick, the peak stress in the relieved zone is approximately 5.3 MPa, while that in the concentrated zone is about 21.1 MPa. With the same protective layer thickness (3 m) but a greater protected layer thickness of 10 m, the peak stress in the relieved zone reaches about 5.8 MPa, whereas that in the concentrated zone decreases to around 20.8 MPa. Therefore, as the thickness of the protected layer increases, the peak stress in the relieved zone gradually rises, while the peak stress in the concentrated zone gradually declines.

4.4. SERVICE LIFE OF PROTECTIVE LAYERS

According to current standards, the pressure relief period shall commence upon completion of the protective seam extraction and should not be exceeded when mining the protected seam. The pressure relief period shall be determined comprehensively through theoretical analysis, field monitoring, or engineering analogy. When the protective seam is extracted using the total caving method, the pressure relief period shall not exceed three years. When the total backfill method is adopted, the pressure relief period shall not exceed two years. Considering that after the extraction of the protective seam, the overlying strata collapse is relatively incomplete at the edges of the goaf, whereas the goaf center exhibits a higher degree of compaction and stress recovery. Consequently, if the gateways of the protected seam working face are located beneath the edge of the protective seam goaf, the effective duration of pressure relief provided by the protective seam may extend beyond three years, as illustrated in Figure 16.

5. ENGINEERING PRACTICE OF PROTECTIVE SEAM MINING FOR ROCK BURST PREVENTION

5.1. GEOLOGICAL AND MINING CONDITIONS

The planned new mine in western China targets the No. 2-2 and No. 3-1 coal seams as its primary mining horizons. The No. 2-2 seam has an average burial depth of approximately 680 m and an average thickness of 3.4 m, while the No. 3-1 seam lies at an average depth of about 740 m with an average thickness of 6.3 m. The No. 2-2 seam is located stratigraphically about 60 m above the No. 3-1 seam. Based on burst proneness assessment, both seams are identified as having weak burst proneness.

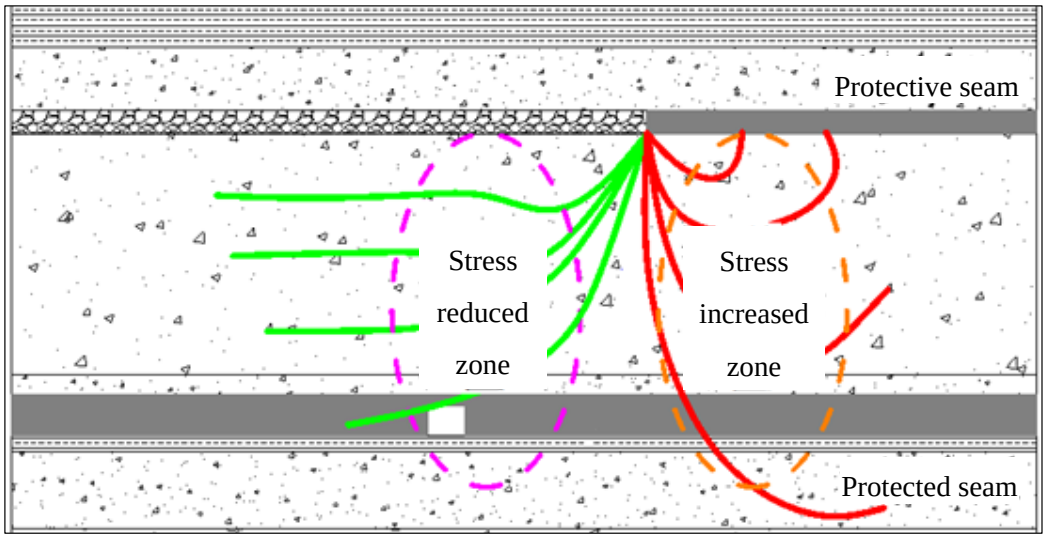

Fig. 16 The staggered internal arrangement scheme of roadways for protective seam mining.

5.2. DESIGN OF PROTECTIVE LAYER MINING FOR ROCK BURST PREVENTION

To effectively mitigate rock burst risks at the source and ensure safe production in later stages, it is necessary, from the perspective of regional rock burst prevention, to formulate a rational mining design scheme for the protective seam in this newly constructed mine.

The maximum interlayer spacing between the No. 2-2 and No. 3-1 coal seams is approximately 40 m. Based on the theoretical calculation of the maximum protective range for protective seam mining derived in Chapter 2, which is about 50 m, it can be theoretically considered that mining the No. 2-2 seam as a protective layer can effectively achieve rock burst prevention for the subsequent mining of the No. 3-1 seam. Chapter 3 validates the pressure relief, shock absorption, and energy absorption effects of protective seam mining through numerical simulation methods, with the main conclusions summarized as follows: 1. After mining the No. 2-2 seam, the stress level at the No. 3-1 seam is reduced by approximately 70 %; 2. After mining the No. 2-2 seam, the stress and displacement responses at the No. 3-1 seam under dynamic loading are significantly reduced; 3. After mining the No. 2-2 seam, the strain energy accumulation state within the protected seam range is effectively improved. Chapter 4 conducts a comparative study on different key parameters of protective seam mining. The results indicate that the actual interlayer spacing, lithology of the interburden, and the thicknesses of the protective and protected seams in this mine can ensure that protective seam mining achieves good pressure relief and rock burst prevention effects. The aforementioned research findings demonstrate the feasibility and scientific rationale of using the No. 2-2 seam as the protective layer.

In terms of specifically guiding the design of the protective seam mining plan, this is reflected in the roadway layout plan and the mining sequence plan. The roadway layout plan is based on the protected range of the protected seam obtained through the aforementioned numerical simulations, including both horizontal and vertical positions, with the aim of ensuring that the working face of the protected seam is located in the area of minimum stress. The determination of the mining sequence, on the other hand, needs to consider the optimal timing for protective seam mining to ensure that the protected seam working face still maintains effective pressure relief and rock burst prevention effects during its extraction period.

5.2.1. ROCK BURST PREVENTION LAYOUT FOR PROTECTIVE LAYER MINING

Given the close proximity of the 2-2 and 3-1 coal seams, and considering the relatively thin thickness of the 2-2 seam which leads to a limited scope of mining-induced disturbance, it is advisable to adopt downward mining by extracting the 2-2 seam first as a protective layer for the 3-1 seam. Based on the actual geological conditions of the 2-2 and 3-1 coal seams, two joint alternating mining plans are proposed: the same-wing dual-seam joint alternating mining plan and the two-wing dual-seam joint alternating mining plan.

1. Coordinated Alternate Mining Scheme for Twin Coal Seams on the Same Flank

In this scheme, the central main roadway is oriented parallel to the western mine boundary, while the working faces on both flanks are arranged perpendicular to the central main roadway. The first mining panel of the protective seam is located in the northwest area of the mine. The first mining panel of the protected seam is situated directly beneath that of the protective seam, with its intake airway, return airway, open-off cut, and stopping line all offset inward relative to the corresponding entries of the protective seam panel. After the full extraction of panel 2-201, mining proceeds to panel 2-202. Once

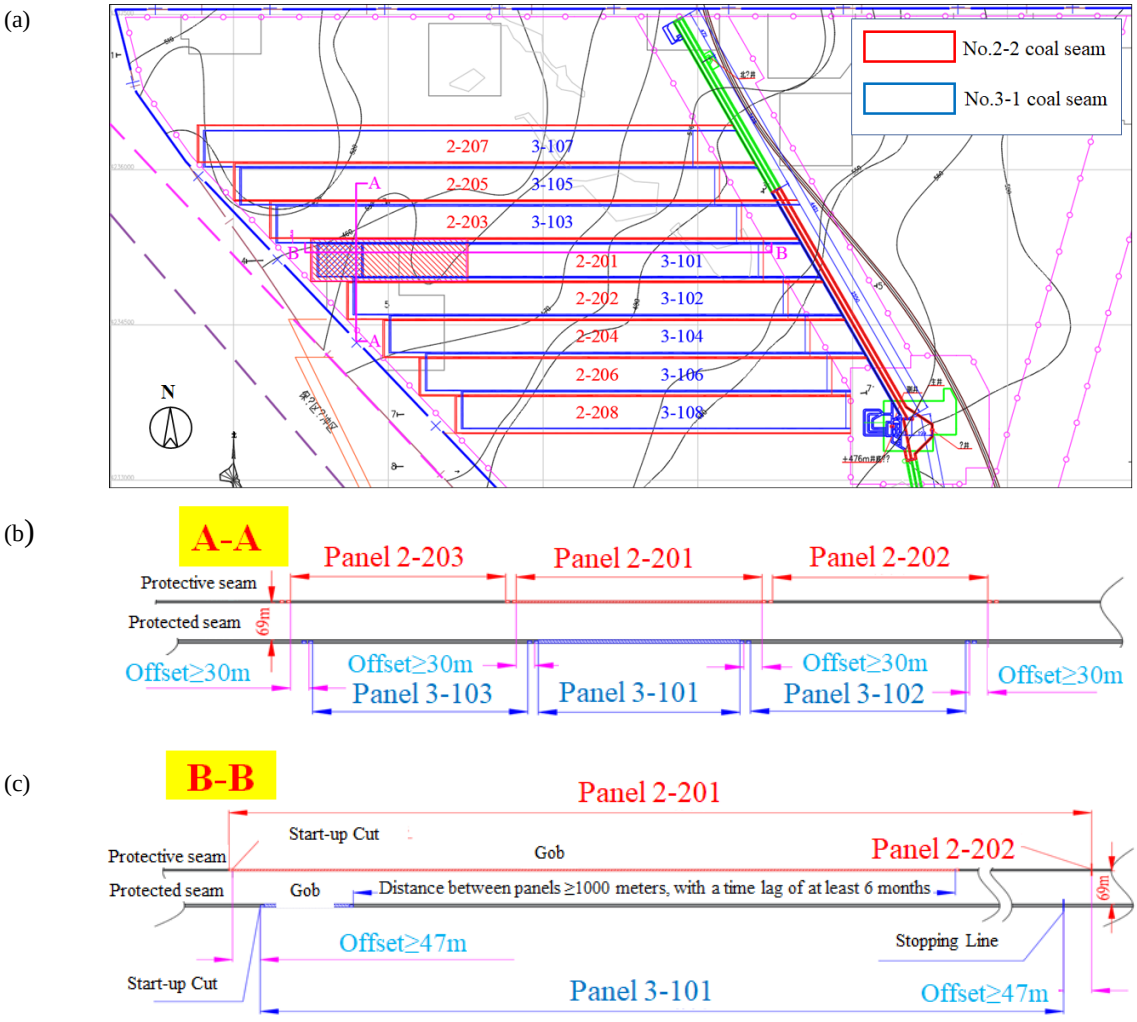

Fig. 17 Coordinated alternate mining of coseams.

panel 2-202 and panel 3-101 are separated by a distance of 1000 m, extraction of panel 3-101 begins and this spacing is maintained throughout. Following the completion of panel 3-101, mining advances to panel 3-102. Subsequent panels are then alternately extracted in a skip-mining sequence, alternating between the northern and southern sides of the first mining panels, as described above. A schematic layout of the arrangement is shown in Figure 17. The 3-1 coal seam working face maintains a lag distance of over 1000 meters behind the 2-2 coal seam working face, with the goaf of the latter having achieved stability for a period exceeding six months.

2. Dual-Wing Dual-Seam Combined Alternate Mining Scheme

In Scheme 2, the layout of the first mining faces in the protective and protected seams remains the same as in Scheme 1. The difference lies in the arrangement of the subsequent face, which is positioned on the right flank of the central roadway. Subsequent working faces then retreat alternately between the left and right sides of the central roadway in the sequence described above. A schematic of the layout is shown in Figure 18.

5.2.2. STAGGERED DISTANCE FOR ROADWAY LAYOUT IN PROTECTIVE LAYER MINING

Under protective layer mining conditions, a reasonable offset distance for the inclined working face should consist of two components: first, the protective offset distance provided by the protective layer; second, the combined width of the entry reserved for the next working face and the width of the section coal pillar.

1. Offset distance within the protective range of the working face

Based on the principle for determining the protective range of the protective layer, the pressure relief angles δ_3 and δ_4 are taken as 75°. With the maximum interburden spacing calculated as 69 m, the first component of the offset distance within the protective range should be L_1=69/tan75°=18.5 m. The second component corresponds to the width of the entry reserved for the subsequent working face and the width of the section coal pillar. Assuming the widths of the intake and return airways are d_1 and the section coal pillar between two adjacent working faces is d_2, this part of the width is $L_2=d_1+d_2$.

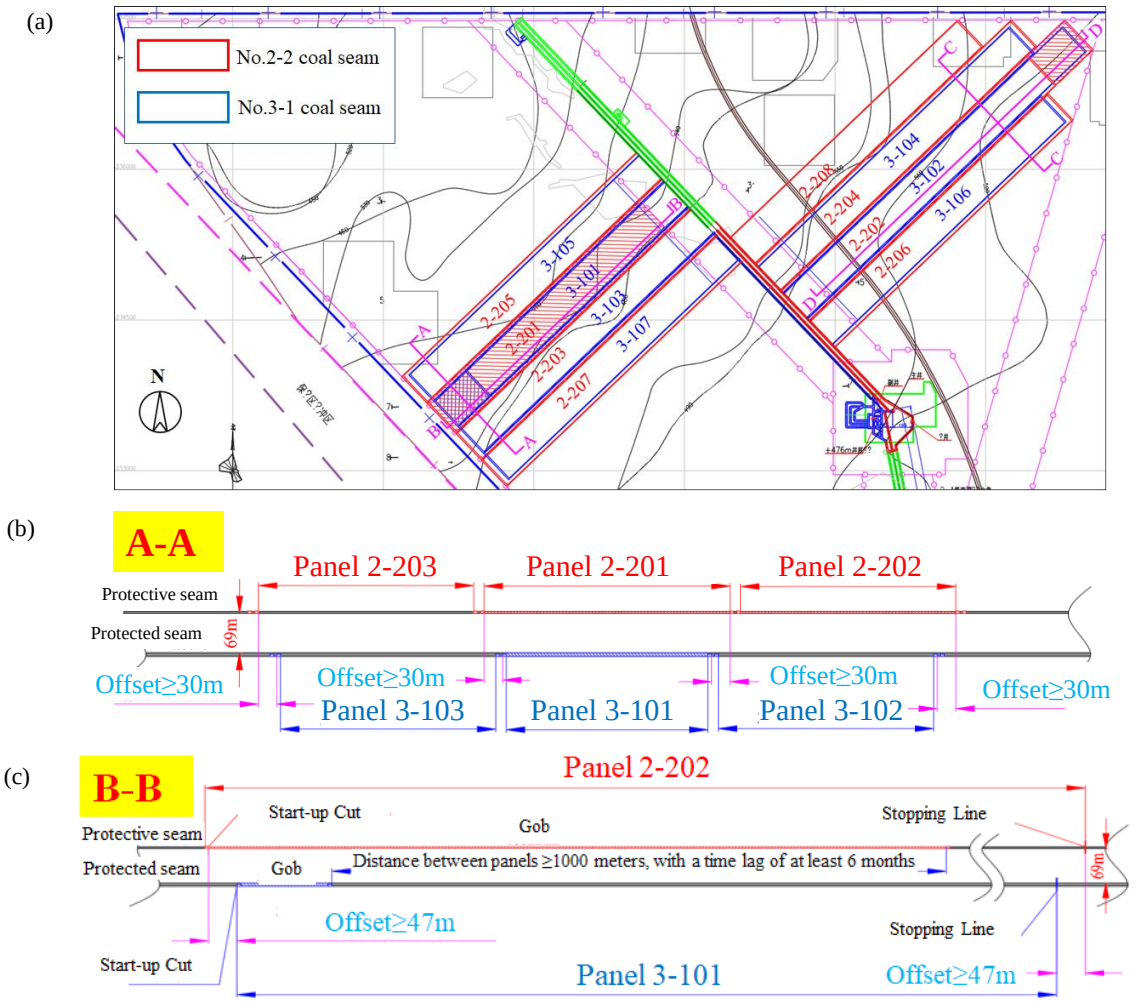

Fig. 18 Combined alternating extraction strategy for dual-seam mining with a double-wing layout.

In summary, the inclination offset of working faces for the combined mining of the protective seams 2-2 and 3-1 is given by:

$$L=L_1+L_2=18.5+d_1+d_2 \quad (3)$$

Where,

L denotes the inclination offset between the working faces in seams 2-2 and 3-1, in m;

L_1 is the protective offset of the protective layer, with L_1=69/tan 75°=18.5 m;

L_2 represents the sum of the entry width d_1 reserved for the next stage working face and the width d_2 of the section coal pillar, i.e., $L_2=d_1+d_2$, in m.

Among the aforementioned parameters, assuming the width of the headgate and tailgate for the working face is set as 5.5 m, and the width of the inter-panel coal pillar between two adjacent working faces is 5.0 m, then L = 18.5 + 5.5 + 5.0 = 30 m. Consequently, in the dip direction, the gateways of the 3-1 coal seam (the protected seam) working face must be offset by at least 30 m from those of the 2-2 coal seam (the protective seam) working face. In field applications, this offset should be adjusted according to the actual roadway width and the designed width of the inter-panel coal pillar.

2. Strike direction offset within the protective range

According to the principle for determining the protective range of the protective seam, the relief angle (δ_5) at the starting line and stopping line of the panel ranges from 56° to 60°. For conservative design, 56° is adopted. Given an interburden thickness of 69 m between the seams, the required offset within the protective range is calculated as 69 / tan 56° ≈ 46.54 m, which is rounded up to 47 m. Therefore, both the starting line and the stopping line of the 3-1 coal seam panel should be offset inward by at least 47 m relative to those of the 2-2 coal seam panel.

5.2.3. EVALUATION OF ALTERNATIVE SCHEMES

Based on the regional rock burst prevention principle and panel layout principle for the combined extraction of the 2-2 and 3-1 coal seams, two alternative schemes are proposed: the same-wing double-seam combined alternate mining and the double-wing double-seam combined alternate mining. Both Scheme 1 and Scheme 2 not only ensure the avoidance of misalignment in certain areas of the setup room and stopping line within the same coal seam, but also guarantee that all working faces in the 3-1 coal

seam remain within the effective protective range, thereby achieving satisfactory protection outcomes. Meanwhile, by optimizing the panel layout, the loss of most triangular coal blocks in the west-wing panels is avoided, contributing to the conservation of coal resources. Under the premise of reasonably regulating the mining speed, the working faces in the 3-1 coal seam can be maintained within the effective pressure relief period. Compared with Scheme 1, Scheme 2 employs leapfrog mining on both sides of the central roadway, which effectively mitigates the issue of concentrated mining and excavation activities. Therefore, Scheme 2 is considered the preferable option.

6. CONCLUSIONS

Through theoretical analysis, this study systematically proposes the rock burst prevention effect of protective coal seam mining characterized by pressure relief, vibration dampening, and energy absorption. Using numerical simulations, the influence of different spatio-temporal parameters on the effectiveness of rock burst prevention by protective seam mining was investigated. Finally, the research findings were applied in field practice, validating the rationality of the proposed effect. The main findings are summarized as follows:

1. Protective layer mining, as the most effective strategic regional measure for rock burst prevention, demonstrates significant rock burst control effects within its effective protection range and duration. These effects include substantial stress reduction in the protected layer, decreased occurrence of strong mining-induced seismicity, and effective absorption of strain energy.
2. Numerical results indicate that under certain conditions, the stress release rate at the protected layer can reach up to 25% after protective layer mining. Stress concentration zones are observed at the interaction regions between the protective layer, the protected layer, and the interlayer strata, primarily associated with lateral stress concentration within the interlayer rock. Protective layer mining mitigates the impact of mining-induced seismicity on the stress and displacement of the protected layer and effectively absorbs strain energy during the mining process.
3. A smaller interlayer distance leads to a more pronounced reduction in vertical stress within the protected layer, but results in higher stress concentration within the stress elevation zone. When the interlayer lithology is soft rock, the critical relief angle is larger than that for hard rock undergoing plastic failure. With increasing protective layer thickness, the peak stress in the pressure relief zone gradually decreases, while the peak stress in the pressure increase zone gradually rises. The opposite trend is observed with increasing protected layer thickness.
4. Taking a planned mine as an example, two different protective layer mining schemes were designed based on the occurrence conditions of the coal seams. Through comparative analysis, the optimal scheme was determined to serve as the overall guideline for subsequent rock burst prevention work.

ACKNOWLEDGMENT

This research was carried out by the funded projects: Basic Science (Natural Science) Research Projects in Higher Education Institutions of Jiangsu Province (Grant ID 25KJB440002). Open Research Project Funding from the National Key Laboratory of Coal Fine Exploration and Intelligent Development at China University of Mining and Technology (Grant ID SKLCRSM24KF019). Open Research Grant of Key Laboratory of Coal Mine Rock Burst Prevention & Control Technology and Equipment, National Mine Safety Administration (Grant ID SDEGIF-FC202501). The Taishan Industrial Experts Program (Grant ID tscx202408130).

CONFLICT OF INTEREST

The authors declare that the research was conducted in the absence of any commercial or financial relationships that could be construed as a potential conflict of interest.

REFERENCES

Cook, N.G.W.: 1965, A note on rockbursts considered as a problem of stability. J. South Afr. Inst. Min. Metall., 65, 8, 437–446.

Dai, L., Zhao, X., Pan, Y., Luo, H., Gao, Y., Wang, A., Ding, L. and Li, P.: 2025, Microseismic criterion for dynamic risk assessment and warning of roadway rockburst induced by coal mine seismicity. Eng. Geol., 357, 108324. DOI: 10.1016/j.enggeo.2025.108324

Dou, L., Tian, X., Cao, A., Gong, S., He, H., He, J., Cai, W. and Li, X.: 2022, Present situation and problems of coal mine rock burst prevention and control in China. J. China Coal Soc., 47, 1, 152–171, (in Chinese). DOI: 10.13225/j.cnki.jccs.yg21.1873

Ellsworth, W.L.: 2013, Injection-induced earthquakes. Science, 341, 6142, 1225942. DOI: 10.1126/science.1225942

Fang, S., Zhu, H., Huo, Y., Zhang, Y., Wang, H., Li, F. and Wang, X.: 2021, The pressure relief protection effect of different strip widths, dip angles and pillar widths of an underside protective seam. Plos One, 28, 16, e0246199. DOI: 10.1371/journal.pone.0246199

Jiang, F., Liu, Y., Liu, J., Zhang, M., Du, J., Sun, W. and Zhang, W.: 2019, Pressure-releasing mechanism of local protective layer in coal seam with rock burst. Chin. J. Geotech. Eng., 41, 02, 368–375, (in Chinese). DOI: 10.11779/CJGE201902016

Jiao, Z., Tao, G., Wang, H. and Lu, Z.: 2017, Overburden strata movement and fissure evolution in lower protective layer in Jincheng mining district. J. Min. Saf. Eng., 34, 01, 85–90, (in Chinese). DOI: 10.13545/j.cnki.jmse.2017.01.013

Liu, H., Cheng, Y., Zhao, C., Zhou, H. and Zhang, Z.: 2010, Classification and judgment method of the protective layers. J. Min. Saf. Eng., 27, 04, 468–474, (in Chinese). DOI: 10.3969/j.issn.1673-3363.2010.04.005

Liu, Y. and Li, G.: 2013, Reliability research of protective layer mining and pressure-relief gas drainage. J. Min. Saf. Eng., 30, 03, 426-431+436, (in Chinese). DOI: CNKI:SUN:KSYL.0.2013-03-021

Noack, K.: 1998, Control of gas emissions in underground coal mines. Int. J. Coal Geol., 35, 1-4, 57–82. DOI: 10.1016/S0166-5162(97)00008-6

Qi, Q., Ji, W., Yuan, J., Cheng, Z. and Liu, X.: 2014, In-situ observation on the floor-connected crack field and its effects on methane extraction. J. China Coal Soc., 39, 08, 1552–1558, (in Chinese). DOI: 10.13225/j.cnki.jccs.2014.9042

Regulations on the Prevention and Control of Rock Burst in Coal Mines: 2019, National Coal Mine Safety Administration. Beijing, (in Chinese).

Sun, Q., Zhang, J., Zhang, Q., Yin, W. and Germain, D.A: 2016, A protective seam with nearly whole rock mining technology for controlling coal and gas outburst hazards: a case study. Nat. Hazards., 16, 3, 1793–1806. DOI: 10.1007/s11069-016-2512-9

Tian, K., Sun, W. and Wei, Er.: 2013, Determination of protection range for mining upper protective layers and its numerical simulation. J. Liaoning Tech. Univ. (Nat. Sci. Ed.), 32, 01, 7–13, (in Chinese). DOI: CNKI:SUN:FXKY.0.2013-01-003

Tu, M. and Fu, B.: 2011, Analysis of the effect of key strata structure on relief-pressure mining in protective seam. J. Min. Saf. Eng., 28, 04, 536–541, (in Chinese). DOI: 10.3969/j.issn.1673-3363.2011.04.007

Wang, L., Liu, S., Cheng, Y., Yin, G., Zhang, D. and Guo, P.: 2017, Reservoir reconstruction technologies for coalbed methane recovery in deep and multiple seams. Int. J. Min. Sci. Technol., 27, 2, 277–284. DOI: 10.1016/j.ijmst.2017.01.026

Wang, Z., Yang, R. and Zhang, Y: 2011, Study on protection layer mining effect evaluation indexes and their applications. China Saf. Sci. J., 21, 10, 58–63, (in Chinese). DOI: 10.16265/j.cnki.issn1003-3033.2011.10.023

Wu, X.: 2012, Pressure-relief, vibration-damping and energy-absorbing effects of protective coal seam and its application. Xuzhou, China University of Mining and Technology, (in Chinese).

Wu, X., Dou, L., Lyu, C. and Zheng Y.: 2012, Study on upper liberated seam mining to pressure releasing function of low seam. Coal Sci. Technol., 40, 3, 28–31, 61, (in Chinese). DOI: 10.13199/j.cst.2012.03.33.wuxq.015

Xie, H., Zhou, H., Liu, J., Gao, F., Zhang, R., Xue, D. and Zhang, Y.: 2011, Mining-induced mechanical behavior in coal seams under different mining layouts. J. China Coal Soc., 36, 07, 1076–1074, (in Chinese). DOI: 10.13225/j.cnki.jccs.2011.07.025

Yang, W., Lin, B., Qu, Y., Li, Z., Zhai, C., Li, J. and Zhao, W.: 2011, Stress evolution with time and space during mining of a coal seam. Int. J. Rock Mech. Min. Sci., 48, 7, 1145–1152. DOI: 10.1016/j.ijrmms.2011.07.006

Yardimci, A.G. and Murat Karakus, A.: 2020, A new protective destressing technique in underground hard coal mining. Int. J. Rock Mech. Min. Sci., 130, 104327. DOI: 10.1016/j.ijrmms.2020.104327

Yuan, L.: 2008, Key technique of safe mining in low permeability and methane-rich seam group. Chin. J. Rock Mech. Eng., 27, 7, 1370–1379, (in Chinese).

Yuan, L. and Xue, S.: 2014, Defining outburst-free zones in protective mining with seam gas content-method and application. J. China Coal Soc., 39, 09, 1786–1791, (in Chinese). DOI: 10.13225/j.cnki.jccs.2014.8019

Yin, W., Miao, X., Zhang, J. and Zhong, S.: 2017, Mechanical analysis of effective pressure relief protection range of upper protective seam mining. Int. J. Min. Sci. Technol., 27, 3, 537–543, (in Chinese). DOI: 10.1016/j.ijmst.2017.03.021

Zhou, C., Chen, Y., Hu, R. and Yang, Z: 2023, Groundwater flow through fractured rocks and seepage control in geotechnical engineering: Theories and practices. J. Rock Mech. Geotech. Eng., 15, 1, 1–36. DOI: 10.1016/j.jrmge.2022.10.001